Infection and Drug Resistance Dovepress

Open Access Full Text Article

CLINICAL TRIAL REPORT

Quantifying the Long and Short Axes of the External Iliac Lymph Nodes Using Dual-Energy Computed Tomography: A Potential Diagnostic Approach for Periprosthetic Joint Infection – A Prospective Study

Yaji Yang[1–3,*], Haotian Zhou[1–3,*], Runxing Kang[1–3], Chen Zhao[1–3], Jia Li[4], Feilong Li[1–3], Yidong Shen[1–3], Yuelong Chen[5], Wei Huang[1–3], Leilei Qin[1–3]

[1]Department of Orthopaedic Surgery, The First Affiliated Hospital of Chongqing Medical University, Chongqing, People's Republic of China; [2]Chongqing Municipal Health Commission Key Laboratory of Musculoskeletal Regeneration and Translational Medicine, Chongqing, People's Republic of China; [3]Orthopaedic Research Laboratory of Chongqing Medical University, Chongqing, People's Republic of China; [4]Department of Radiology, The First Affiliated Hospital of Chongqing Medical University, Chongqing, People's Republic of China; [5]Hospital of Chongqing University, Chongqing University, Chongqing, People's Republic of China

*These authors contributed equally to this work

Correspondence: Wei Huang; Leilei Qin, Department of Orthopaedics, the First Affiliated Hospital of Chongqing Medical University, Chongqing, 400016, People's Republic of China, Email huangwei68@263.net; qinleilei@stu.cqmu.edu.cn

Purpose: Periprosthetic joint infection (PJI) is a severe complication following joint replacement surgery, and there is a current lack of rapid, accurate, and non-invasive diagnostic methods. This study aims to assess the effectiveness of using dual-energy computed tomography (DECT) to quantify the maximum long and short axes of the external iliac lymph nodes (LNs) as a diagnostic tool for PJI.

Patients and Methods: In this prospective controlled study, 112 patients undergoing total hip or total knee revision surgery were enrolled. All patients underwent preoperative DECT scanning to measure the maximum long and short axes of the external iliac LNs on the affected side. The diagnostic value of lymph node size for PJI was assessed using receiver operating characteristic curves.

Results: The AUC (Area Under the Curve) quantifies the diagnostic method's ability to distinguish between positive and negative outcomes in this study. A value closer to 1.0 indicates better discriminatory performance. Compared to erythrocyte sedimentation rate (Area Under the Curve (AUC) = 0.834), percentage of polymorphonuclear leukocytes (AUC = 0.621), and C-reactive protein (AUC = 0.765), the maximum long axis (AUC =0.895) and maximum short axis (AUC = 0.858) of the external iliac LNs better differentiated PJI from aseptic failure. For diagnosing PJI, the threshold for the maximum long axis of the LNs was 20.5 mm, with a sensitivity of 84.21% and a specificity of 87.84%. For the maximum short axis, the threshold was 8.5 mm, with a sensitivity of 89.47% and a specificity of 82.43%. Combining the maximum long and short axes of the external iliac LNs enhanced the diagnostic accuracy for PJI.

Conclusion: Measuring the long and short axes of external iliac LNs using DECT is an effective diagnostic approach for PJI, aiding in the differentiation between PJI and aseptic failure following joint replacement surgery.

Keywords: periprosthetic joint infection, diagnosis, dual-energy CT, lymph nodes

Introduction

Periprosthetic joint infection (PJI) following joint replacement surgery is one of the most catastrophic complications that clinicians must address.[1] Although the incidence of PJI is only around 2–3%, it is a significant cause of joint revision surgery, accounting for approximately 15% of cases.[2,3] PJI imposes significant physical, psychological, and economic burdens on patients and presents substantial challenges to the healthcare system. The accurate and timely diagnosis of PJI is crucial for surgeons in determining the appropriate method and timing for prosthesis revision surgery.[4] Pathogens can suppress and evade recognition and destruction by the host immune system, and low-virulence pathogens often do not

Received: 24 September 2024
Accepted: 12 December 2024
Published: 17 December 2024

trigger a strong inflammatory response. This results in subtle infection symptoms and a slow disease progression, blurring the distinction between PJI and aseptic failure.[5,6] Therefore, the search for an accurate and rapid diagnostic method for PJI is a key challenge for clinicians.

Although international consensus on PJI diagnosis is continually updated to incorporate new technologies and biomarkers, a unified "gold standard" remains elusive. Traditional serological inflammatory markers, such as C-reactive protein (CRP) and erythrocyte sedimentation rate (ESR), are widely accepted and have been incorporated into the Musculoskeletal Infection Society (MSIS) diagnostic criteria due to their simplicity and ease of use.[7] However, as non-specific inflammatory markers, their diagnostic specificity for PJI is often suboptimal.[8] In our previous studies, synovial fluid biomarkers, such as interleukin-6 and α-defensin, were effective in distinguishing PJI from aseptic failure patients; however, there remains a risk of dry tap, leading to test failure.[5,9] Additionally, synovial fluid inflammatory cytokine levels have limited ability to differentiate between PJI and autoimmune diseases such as gout.[10] Moreover, invasive surgical procedures carry technical challenges and the risk of infection, preventing widespread use in primary care settings and limiting the effectiveness of early infection screening. Therefore, there is an urgent need for clinicians to find a simple, non-invasive, and rapid diagnostic method for PJI.

The lymphatic system, as a critical component of the immune system, can detect and respond to peripheral inflammatory stimuli and infections.[11] During infection, lymph nodes (LNs) filter lymphocytes from the draining region and scan for pathogens, antigens, or inflammatory factors, initiating T-cell and B-cell immune responses, which can ultimately lead to lymph node enlargement.[12] LNs are highly sensitive to infection, with their size rapidly increasing within 2–3 days of infection and returning to normal within weeks after the infection is fully controlled.[13] Therefore, lymph node enlargement has become a critical indicator in the observation of infections or immune diseases.[13,14] Studies have shown that in patients with malignancies, using the maximum short axis of LNs as a diagnostic criterion can accurately diagnose lymphatic metastasis.[15,16] In our previous study using ultrasound to examine inguinal LNs, we found that PJI leads to significant lymph node enlargement, which normalizes as the infection is controlled; the maximum long axis of LNs proved effective in diagnosing PJI.[17] However, because inguinal LNs are close to the skin and external environment, they are susceptible to interference from superficial infections, trauma, and other factors, leading to potential bias in the results.[18] We sought to identify soft tissue structures more closely associated with the pathophysiological changes in the joint and surrounding tissues. The external iliac LNs, located near the external iliac vessels, constitute a significant lymph node group in the pelvic region. They receive lymphatic drainage from the lower limb LNs, including the inguinal nodes, as well as from the pelvic region.[19] The external iliac LNs not only reflect changes in the lymphatic drainage area of the inguinal nodes but also monitor infections in the hip joint and deep pelvic tissues. Studies have found that external iliac LNs are significantly enlarged in patients with PJI after hip replacement surgery, and this enlargement is an important independent predictor of PJI.[20] However, no studies have examined the specific changes in the long and short axes of the external iliac LNs or their diagnostic thresholds for PJI.

Imaging examinations are routine diagnostic tools for orthopedic surgeons, but their effectiveness in diagnosing PJI varies. While X-rays provide anatomical information about bones and joints, their diagnostic performance for PJI is relatively poor.[21] Magnetic resonance imaging (MRI) has shown good diagnostic efficacy for PJI; however, its imaging is often affected by metal artifacts.[22] The three-phase bone scan is a simple and widely used radionuclide imaging technique for diagnosing PJI. However, literature indicates that it exhibits high sensitivity but low specificity for PJI diagnosis.[23] Fluorodeoxyglucose positron emission tomography (FDG-PET) using fluorodeoxyglucose as a tracer is limited by its cost, contraindications such as tracer allergies, and concerns regarding its diagnostic efficacy.[24] Currently, artificial intelligence (AI), particularly convolutional neural networks (CNNs), is being applied to medical imaging diagnostics. AI tools based on CNNs have demonstrated promising value in analyzing three-phase bone scan images for PJI detection.[23] However, given the contraindications associated with imaging agents and the inherent limitations of the diagnostic performance of three-phase bone scans, there remains room for improvement in AI-assisted imaging diagnostic tools. Therefore, this study aims to explore an imaging technique that is fast, has fewer contraindications, and exhibits high diagnostic performance. Such a technique would not only facilitate clinical practice but also provide a foundation for developing novel AI-based imaging tools for PJI diagnosis. Dual-energy computed tomography (DECT) acquires two different sets of imaging data by emitting X-rays at two different energy levels. With advanced software and

techniques, it effectively reduces prosthesis artifact interference, making it highly valuable in diagnosing PJI.[25,26] Compared to conventional computed tomography (CT) and ultrasound, DECT offers superior soft tissue differentiation, accurately identifying bone tissue, blood vessels, and LNs, leading to more precise data. Our previous research found that using DECT iodine maps to quantify inflammation in the periprosthetic soft tissue provided good sensitivity and specificity for differentiating PJI.[27] Compared to MRI, DECT offers advantages such as faster imaging, lower cost, and fewer contraindications.

Therefore, in this prospective controlled study, we investigated a novel approach for diagnosing PJI by detecting the long and short axes of external iliac LNs using DECT, without incurring additional costs or causing harm to patients. Our objectives were to: 1) determine whether enlargement of the external iliac LNs on the affected side can differentiate between PJI and aseptic failure as the cause for revision surgery; and 2) establish diagnostic thresholds for PJI based on the maximum long and short axes of the external iliac LNs on the affected side.

Materials and Methods

Patient Cohort and Characteristics

In this prospective cohort study, conducted from March 1, 2021, to July 31, 2024, we enrolled 128 patients who required total hip or total knee revision surgery due to PJI or aseptic failure. All participants signed informed consent before enrollment, and the study was approved by the Institutional Review Board and registered with the Chinese Clinical Trial Registry (No. 2021–258; No. ChiCTR2100050785).

Patients with any type of skin ulcer or hematoma, recent trauma or dislocation (within 2 weeks), extra-articular infections of the lower limbs or sexually transmitted diseases, inflammatory arthritis (such as rheumatoid arthritis and gout), malignancies (lymphoma, lower limb skin cancer, gynecological tumors, bladder cancer, etc)., lower limb vascular diseases (such as embolism and inflammation), or those receiving immunotherapy were excluded. We excluded patients with recent trauma or dislocation (within two weeks) for the following reasons: acute inflammatory responses in local tissues typically lead to systemic lymphatic drainage dysfunction within 24 hours post-trauma and gradually recover over 7–14 days.[28] Studies have shown that aseptic lymph node swelling generally resolves within two weeks.[29–31] Therefore, this exclusion criterion was established to avoid potential non-specific swelling of the external iliac lymph nodes caused by factors unrelated to PJI, thereby minimizing their impact on the study results. A total of 16 patients were excluded: 3 with rheumatoid arthritis, 2 with gout, 1 with lower limb vascular embolism, 4 with malignancies, 3 with lower limb ulcers, 2 with a history of trauma within 14 days, and 1 with prostatitis. Ultimately, 112 patients were included in this study. Participants were divided into an aseptic failure group and a PJI group based on the bacterial culture results from joint and surrounding tissue samples. The aseptic group included cases undergoing total hip or total knee revision surgery for non-infectious reasons, such as aseptic loosening, wear, instability, and malalignment. Patients with positive microbial cultures were classified into the PJI group. Pathogen detection was conducted under strict sterile conditions. All cultures were performed prior to the initiation of antibiotic treatment to prevent interference. Samples were collected preoperatively via joint fluid aspiration and intraoperatively from at least three sites, including joint fluid, periprosthetic soft tissue, and bone tissue. To improve pathogen detection rates, we adopted a protocol based on Cao's study, where removed prosthetic components and surrounding soft tissues were processed directly using ultrasound under laminar airflow in the operating room.[32] The processed specimens were then used for pathogen detection. Detection methods included standard bacterial cultures (from tissue or synovial fluid), specialized cultures (eg, for tuberculosis and fungi), pathological examination, polymerase chain reaction, gene chip analysis, nucleic acid probe technology, and next-generation sequencing. Bacterial cultures were typically incubated for 24–48 hours and extended up to 14 days for intraoperative specimens. A positive result was confirmed only when the same pathogen was identified in multiple specimens, effectively minimizing the risks of false positives and contamination. Additionally, postoperative specimens testing positive for bacterial cultures were also classified as PJI cases.

We recorded the following baseline data for the patients: age, gender, and body mass index (BMI). After admission, venous blood was collected to analyze serum ESR and CRP levels. To prevent dry taps, ultrasound-guided aspiration

with puncture needles was performed preoperatively to collect joint fluid from patients for polymorphonuclear neutrophil percentage (PMN%) analysis and culture.

Image Acquisition and Analyses

All patients underwent DECT (Somatom Definition Flash; Siemens Healthineers, Erlangen, Germany) scanning of the pelvis and inguinal region in a supine position, with arms elevated, thighs internally rotated, and toes touching each other. CT images were acquired using the following parameters: pitch 0.6; rotation time 0.4 seconds; Collimation 40×0.6 mm; tube voltage 80 kV, 140 kV. Three radiologists with experience in orthopedic imaging independently analyzed the images of the external iliac LNs on the affected side without knowledge of the patients' clinical information, recording lymph node characteristics such as the short and long axis diameters. (Figures 1 and 2) The maximum long axis and short axis diameters of the affected external iliac LNs for each patient were analyzed as measured by the three radiologists, and the average values were calculated. Consistency among the three radiologists was assessed using the intraclass correlation coefficient (ICC), evaluating their agreement in measuring the maximum long axis and short axis diameters of the external iliac LNs.

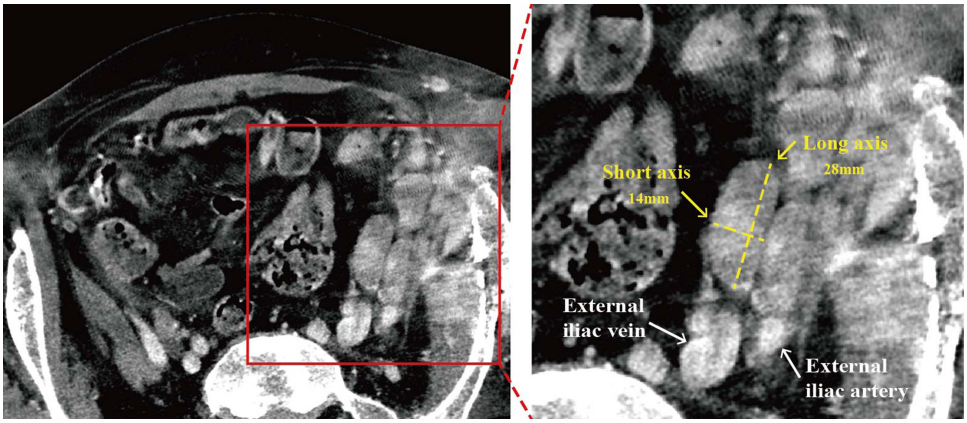

Figure 1 A 56-year-old female with a left Hip prosthesis infection caused by Staphylococcus aureus. The DECT axial view shows the external iliac lymph node on the affected side (left image). The right image illustrates the measurement of the lymph node's long and short axes on the axial DECT scan.
Abbreviations: DECT, dual-energy computed tomography.

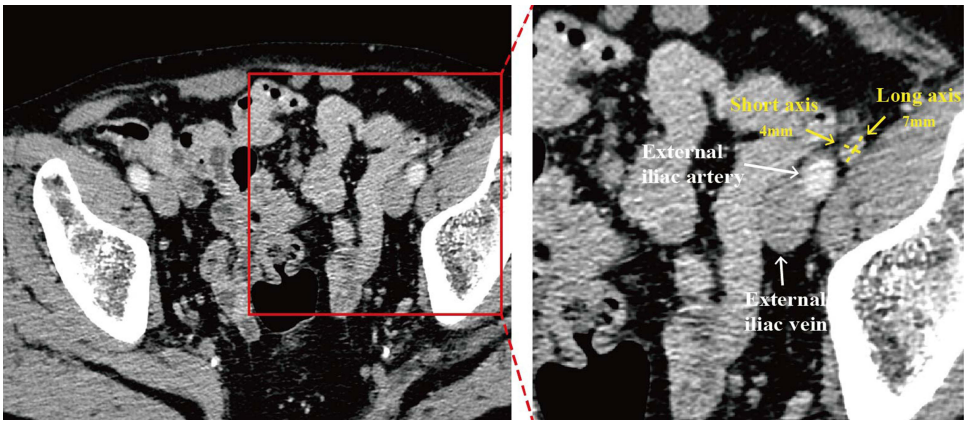

Figure 2 A 66-year-old male with aseptic loosening of the left Hip prosthesis. The DECT axial view shows the external iliac lymph node on the affected side (left image). The right image illustrates the measurement of the lymph node's long and short axes on the axial DECT scan.
Abbreviations: DECT, dual-energy computed tomography.

Data Analyses

Statistical analyses were conducted using SPSS version 25 software (IBM Corp., Armonk, NY, USA) and GraphPad Prism 9.0 software (GraphPad Software, San Diego, CA, USA). Continuous variables are presented as mean ± standard deviation, while categorical variables are expressed as counts and percentages. Continuous variables were analyzed using the Mann–Whitney test, and categorical variables were analyzed using the chi-square test. The ICC was calculated following the methodology described in Terry K Koo's study, using a two-way random-effects model to determine the ICC values and their 95% confidence intervals.[33] Receiver operating characteristic curves (ROC) were plotted using GraphPad Prism 9.0, and the area under the curve (AUC), sensitivity, and specificity were analyzed to assess the diagnostic value of external iliac lymph node size for PJI. The Youden J statistic was used to determine the optimal thresholds for the maximum long and short axes diameters of the external iliac LNs in distinguishing between PJI and aseptic loosening (J = sensitivity + specificity - 1). A *p value* of <0.05 was considered statistically significant.

Results

Table 1 presents the demographic characteristics of the two patient groups. A total of 112 patients were included, of whom 38 were diagnosed with PJI based on pathogen culture results (26 had hip infections and 12 had knee infections), and 74 were revision surgery patients due to aseptic failure. There were no statistically significant differences between the two groups in baseline characteristics, including age (*P value*= 0.322), gender (*P value*= 0.432), height (*P value*= 0.614), weight (*P value*= 0.549), and BMI (*P value*= 0.561). In Table 2, we compared serum ESR, CRP levels, and PMN

Table 1 Demographic Data for the Study Population

	Aseptic (n=74)		PJI (n=38)		*P value*
Age	67.256±11.560		64.684±12.286		0.322
Weight	63.000±9.558		62.486±10.296		0.549
Height	161.540±8.106		162.237±7.975		0.614
BMI	23.634±2.772		23.474±3.333		0.561
Sex					0.432
Man	38	51%	22	58%	
Woman	36	49%	16	42%	

Note: Variables are expressed as mean ± SD, or numbers (percentage). Statistically significant (*P value* ≤ 0.05).
Abbreviations: BMI, body mass index; PJI, periprosthetic joint infections.

Table 2 Analysis of Inflammatory Marker in Patients with PJI and Aseptic Revision

Inflammatory Marker	Group		*P value*
	Aseptic (n=74)	PJI (n=38)	
PMN%			
Median	61.650	65.650	0.036
P25, P75	(54.175, 68.925)	(59.675, 70.150)	
ESR (mm/h)			
Median	23.000	72.000	<0.001
P25, P75	(13.000, 43.000)	(43.500, 90.750)	
CRP (mg/L)			
Median	5.335	21.350	<0.001
P25, P75	(2.532, 11.075)	(11.500, 47.500)	

Note: Statistically significant (*P value* ≤ 0.05).
Abbreviations: CRP, C-reactive protein; ESR, erythrocyte sedimentation rate; PMN%, polymorphonuclear cell percentage; PJI, periprosthetic joint infections.

% in synovial fluid between the aseptic failure group and the PJI group. The results showed significant differences in ESR, CRP, and PMN% between the PJI group and the aseptic failure group. In the PJI group, the median ESR was 72.000 mm/h (range, 43.500–90.750 mm/h), significantly higher than the median ESR of 23.000 mm/h (range, 13.000–43.000 mm/h) in the aseptic group (*P value* <0.001). Additionally, CRP levels in the PJI group were higher than those in the aseptic group, with a median of 21.350 mg/L (range: 11.500–47.500 mg/L) compared to a median of 5.335 mg/L (range, 2.532–11.075 mg/L) in the aseptic group (*P value* <0.001). The PMN% data similarly showed that the median in PJI patients was 65.650% (range, 59.675%-70.150%), higher than the median of 61.650% (range, 54.175%-68.925%) in the aseptic group (*P value* = 0.036).

All images of the external iliac LNs on the affected side were obtained via DECT, and the long and short axis of these LNs were measured to determine their maximum long and short axis values. The ICC results demonstrated good consistency among the three radiologists in measuring the maximum long and short axes of external iliac lymph nodes across both patient groups (PJI and aseptic failure groups): maximum long axis in PJI patients: ICC = 0.937, 95% CI 0.893–0.965; maximum long axis in the aseptic failure group: ICC = 0.91, 95% CI 0.87–0.94; maximum short axis in PJI patients: ICC = 0.842, 95% CI 0.749–0.908; maximum short axis in the aseptic failure group: ICC = 0.75, 95% CI 0.659–0.824 (Figure 3). We then compared the maximum long and short axes of the external iliac LNs on the affected side between the two groups and created box plots. As shown in Figure 3, the external iliac LNs on the affected side were significantly enlarged in the PJI group compared to the aseptic failure group. The median maximum long axis of the external iliac LNs on the affected side in the PJI group was 25.00 mm (range, 23.00–29.50 mm), significantly larger than the median maximum long axis of 15.00 mm (range, 11.00–17.00 mm) in the aseptic failure group (*P value* <0.001). For the maximum short axis, the PJI group's median was 10.50 mm (range, 9.00–14.75 mm), significantly larger than the aseptic revision group's median of 6.00 mm (range, 5.00–14.75 mm) (*P value* <0.001).

To further establish the importance of external iliac LN size in distinguishing PJI from aseptic failure, we used the PJI group as the positive control and the aseptic failure group as the negative control, plotted ROC curves, and determined the optimal thresholds for the maximum long or short axis of the external iliac LN in diagnosing PJI. The maximum long and short axes of the external iliac LNs on the affected side showed strong discrimination between the infection group and the aseptic failure group, with AUCs of 0.895 (95% CI 0.828–0.963) and 0.858 (95% CI 0.781–0.934), respectively. Their diagnostic capability was significantly higher than that of serum ESR 0.834 (95% CI 0.755–0.963), CRP 0.765 (95% CI 0.678–0.852), and synovial fluid PMN% 0.621 (95% CI 0.514–0.728) (Figure 4). As shown in Table 3, CRP levels (optimal threshold = 7.895 mg/L) had an average sensitivity of 84.21% and an average specificity of 67.57%. ESR levels (optimal threshold = 42.500 mm/h) had an average sensitivity of 81.58% and an average specificity of 72.97%.

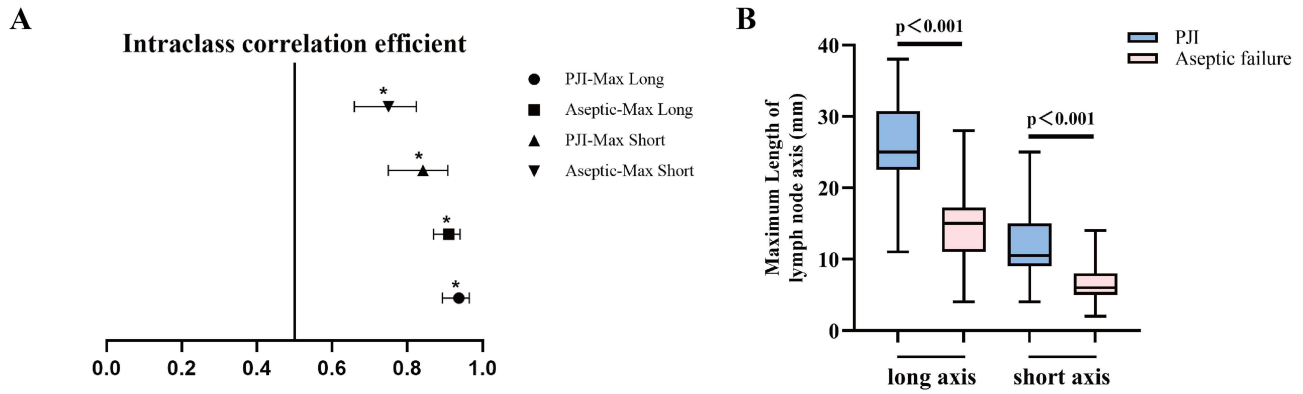

Figure 3 (**A**) The forest plot shows the intraclass correlation coefficient (ICC) and corresponding 95% confidence intervals for the maximum long axes and short axes measurements of external iliac lymph nodes in patients with periprosthetic joint infection (PJI) and aseptic revision, as evaluated by three radiologists. The ICC values, calculated using a two-way random-effects model, assess the consistency among raters. The results indicate high agreement for all measurements, with ICC values exceeding the threshold generally considered reliable (ICC ≥ 0.75). *: P value < 0.001. PJI-long MAX: Maximum long axes of external iliac lymph nodes in PJI patients. Aseptic-long MAX: Maximum long axes of external iliac lymph nodes in aseptic failure patients. PJI-short MAX: Maximum short axes of external iliac lymph nodes in PJI patients. Aseptic-short MAX: Maximum short axes of external iliac lymph nodes in aseptic failure patients. (**B**) Comparison of maximum long and short axes of external iliac lymph nodes between PJI patients and aseptic failure patients.

Abbreviation: PJI, Periprosthetic joint infection.

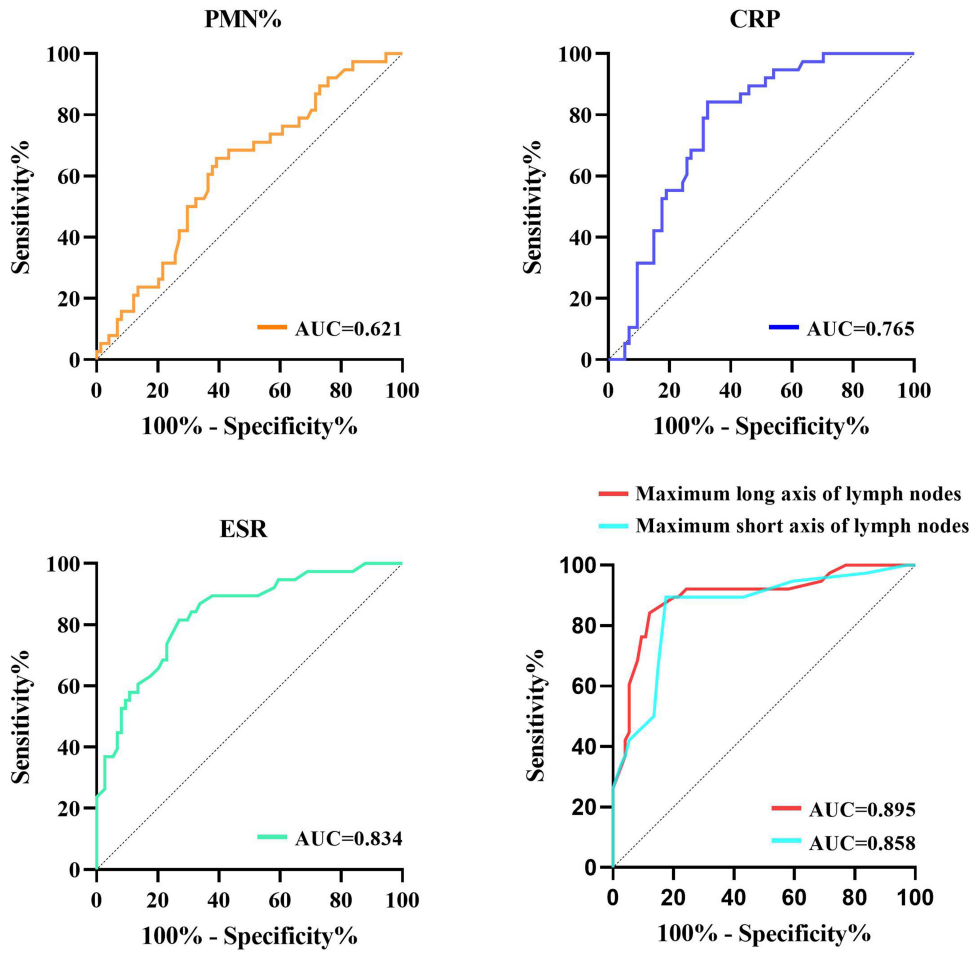

Figure 4 Receiver operating characteristic (ROC) curves and area under curve (AUC) for the four tests to diagnose PJI.
Abbreviations: CRP, C-reactive protein; ESR, erythrocyte sedimentation rate; PMN%, polymorphonuclear cell percentage; PJI, Periprosthetic joint infection.

PMN% levels (optimal threshold = 62.350%) had an average sensitivity of 68.42% and an average specificity of 56.72%. The optimal threshold for the maximum long axis of the external iliac LN in diagnosing PJI was 20.500 mm, with an average sensitivity of 84.21%, an average specificity of 87.84%, and an accuracy of 86.61%. The optimal threshold for the maximum short axis was 8.500 mm, with an average sensitivity of 89.47%, an average specificity of 82.43%, and an accuracy of 84.82%.

Table 3 Performance Parameters of the Four Diagnostic PJI Methods

Parameters	AUC (95% CI)	Cut-off level	Sensitivity (%) (95% CI)	Specificity (%) (95% CI)	PPV (%)	NPV (%)	Accuracy (%)
PMN%	0.621 (0.514–0.728)	62.350	68.42 (52.54–80.92)	56.72 (45.41–67.43)	68.42	56.76	60.71
ESR	0.834 (0.755–0.913)	42.500	81.58 (66.58–90.78)	72.97 (61.91–81.77)	81.58	72.97	75.89
CRP	0.765 (0.678–0.852)	7.895	84.21 (69.58–92.56)	67.57 (56.27–77.14)	84.21	67.57	73.21

(*Continued*)

Table 3 (Continued).

Parameters	AUC (95% CI)	Cut-off level	Sensitivity (%) (95% CI)	Specificity (%) (95% CI)	PPV (%)	NPV (%)	Accuracy (%)
Maximum long axis of lymph nodes	0.895 (0.828–0.963)	20.500	84.21 (69.58–92.56)	87.84 (78.47–93.47)	88.21	87.84	86.61
Maximum short axis of lymph nodes	0.858 (0.781–0.934)	8.500	89.47 (75.87–95.83)	82.43 (72.23–89.44)	89.47	82.43	84.82
Maximum long axis of lymph nodes + Maximum short axis of lymph nodes	N/A	Maximum long axis ≥20.5 Or Maximum minor axis ≥8.5	97.37 (92.28–100.00)	74.32 (64.37–84.28)	97.37	74.32	82.14
	N/A	Maximum long axis ≥20.5 And Maximum minor axis ≥8.5	76.32 (62.80–89.83)	95.95 (91.45–100.00)	76.32	95.95	89.29

Abbreviations: CRP, C-reactive protein; ESR, erythrocyte sedimentation rate; PMN%, polymorphonuclear cell percentage; CI, confidence interval; PJI, periprosthetic joint infections; PPV, positive predictive value; NPV, negative predictive value.

The combined use of the maximum long and short axes in a serial diagnostic approach demonstrated higher accuracy than using either axis alone, though sensitivity was slightly reduced. Although the parallel use of the maximum long and short axes improved sensitivity in diagnosing PJI, its accuracy was somewhat reduced compared to using either axis alone (Table 3).

Discussion

The diagnosis of PJI has consistently been a significant challenge in the field of orthopedics. Low-virulence pathogens and microbial immune evasion mechanisms make it challenging to distinguish the clinical manifestations of PJI from aseptic failure. Despite continuous updates to PJI diagnostic criteria by organizations such as the MSIS and the European Bone and Joint Infection Society, a gold standard for PJI diagnosis remains elusive, limited by insufficient sensitivity and specificity of current criteria, as well as technical and cost-related challenges.[1,34,35] This study is the first to propose measuring the size of the external iliac LNs on the affected side using DECT as a diagnostic strategy for PJI. Our study demonstrates that measuring the maximum long and short axis diameters of the external iliac LNs can serve as effective indicators for diagnosing PJI, outperforming traditional serological markers such as CRP, ESR, and synovial fluid PMN% in diagnostic efficacy. This method capitalizes on the central role of LNs in the immune response, offering a non-invasive, rapid, and reliable diagnostic tool, thus providing new strategies and insights for the clinical diagnosis of PJI.

LNs, as a crucial part of the immune system, often enlarge when the immune system is activated, such as during infections, autoimmune diseases, or tumor development.[14] This pathological enlargement of LNs not only enhances the body's resistance to pathogens but also provides significant reference value for clinical diagnosis and treatment. Studies have shown that LN enlargement can accurately reflect the staging of rectal cancer patients. LN characteristics, such as maximum long axis diameter and maximum short axis diameter, are considered independent predictors of tumor spread.[16,36] Due to the regional drainage characteristics of LNs, localized LN enlargement can specifically indicate the disease status of the local drainage area. Our previous research also demonstrated that localized inguinal LN enlargement can reflect the occurrence of lower limb infections.[17] However, due to the localized drainage characteristics of LNs, selecting the appropriate regional LNs can provide a more comprehensive reflection of changes in the drainage area. The external iliac LNs are arranged along the external iliac artery and primarily receive lymphatic drainage from the inguinal LNs as well as from the bladder, prostate, uterus, and other lymphatic vessels. Compared to inguinal LNs, they have a broader drainage area, allowing for better monitoring of diseases in the lower limbs and pelvis. Additionally, their deeper location helps avoid interference from superficial skin diseases and better reflects the status of deep surrounding tissues of the hip joint.[19] In previous studies, iliac LN enlargement has been identified as an independent clinical variable

associated with PJI.[20] However, metal particles generated from prosthesis wear after joint replacement surgery can also induce aseptic inflammation in the surrounding tissues and lymphocyte proliferation, ultimately resulting in LN enlargement.[37] This can reduce the specificity and sensitivity of diagnosing PJI based solely on LN enlargement. Therefore, we measured the maximum short and long axis of the external iliac LNs on the affected side as a diagnostic standard for PJI, aiming to reduce errors caused by LN enlargement due to aseptic inflammation from metal particles in patients with aseptic failure. Considering that both the long and short axis are important characteristics of LNs, we included both in this study. We found that when the maximum long axes of the external iliac LN reached 20.5 mm, the sensitivity and specificity for diagnosing PJI were 84.21% and 87.84%, respectively; when the maximum short axis reached 8.5 mm, the sensitivity and specificity for diagnosing PJI were 89.47% and 82.43%, respectively. Anatomically, external iliac lymph node swelling is thought to be more closely associated with hip joint infections. However, in our study, all 12 patients with confirmed knee joint PJI showed significant swelling of the external iliac lymph nodes, despite the absence of inflammatory symptoms such as redness, swelling, heat, or pain in areas beyond the knee joint. This suggests that external iliac lymph nodes can reflect lower limb infections, including those of the knee joint. Further research with larger sample sizes is needed to explore whether the degree of external iliac lymph node swelling differs between hip and knee joint infections.

Monitoring changes in the external iliac LNs offers several advantages over traditional serological and synovial fluid biomarker methods. The PJI scoring criteria, such as those from MSIS2011, the International Consensus Meeting(ICM) 2013, and ICM2018, all include the measurement of changes in serological ESR and CRP levels.[1,7,38] However, ESR and CRP, as systemic non-specific markers, can be elevated in both infectious and non-infectious inflammatory conditions. Although their elevation may suggest the possibility of PJI, they cannot be used alone for definitive diagnosis and require other indicators for a combined diagnosis. Additionally, in chronic PJI or PJI caused by low-virulence pathogens, the elevation of ESR and CRP is often not significant, potentially leading to missed diagnoses.[35] In this study, we also found that the accuracy of ESR and CRP in diagnosing PJI is limited, which is consistent with previous studies.[39] In contrast, changes in the external iliac LNs more accurately reflect abnormal conditions in the lymphatic drainage areas of the lower limbs and pelvis, providing regional specificity. Additionally, LNs respond sensitively to infectious diseases, enlarging rapidly in the short term following infection and returning to normal once the infection is controlled.[13] Synovial fluid biomarkers such as IL-6 and IL-4 have high sensitivity and specificity for diagnosing PJI. However, in our previous study, dry tap occurred in some cases, preventing these patients from being fully diagnosed for PJI based on synovial fluid markers, potentially leading to misdiagnosis.[5,40] Additionally, joint aspiration carries a risk of introducing infections. In our study, monitoring changes in the external iliac LNs reduced the need for invasive procedures, avoided patient discomfort and the risk of complications, and made the diagnostic process safer and more convenient.

Radiographic imaging is the cornerstone of orthopedic diagnosis due to its non-invasive nature and ability to reveal the anatomical structures of bones and joints. X-rays are often the first-choice imaging modality for orthopedic surgeons. However, despite their ability to clearly display anatomical features, X-rays lack the specificity and sensitivity needed to diagnose PJI.[21] MRI has shown strong diagnostic capability for PJI in studies. When diagnosing hip joint PJI, MRI demonstrates sensitivity and specificity above 80% for detecting periosteal reactions and capsular edema. However, MRI imaging is highly susceptible to metal artifacts. Even with the use of metal artifact reduction sequences (MARS), MRI image quality often remains unsatisfactory.[22] Additionally, MRI requires lengthy scan times, has numerous contraindications, and is costly. Radionuclide imaging techniques are increasingly being used as adjunctive tests for PJI. Three-phase bone scans are widely used in clinical practice due to their rapid imaging and ability to reflect local inflammation. However, this can make it difficult to distinguish between the causes of increased bone metabolism around implants, such as infection versus aseptic loosening.[41] Fluorodeoxyglucose positron emission tomography, which uses fluorodeoxyglucose as a contrast agent, has shown highly variable results in the literature. Its high cost, along with numerous contraindications such as contrast agent allergies, has prevented it from being widely accepted as a reliable method for diagnosing PJI.[24] CT imaging technology provides high-resolution, three-dimensional structures and is a key technique for LN imaging.[42] However, metal artifacts can interfere with image observation, particularly in the surrounding soft tissue structures. DECT, compared to conventional CT, can more comprehensively characterize attenuation properties and assist in distinguishing different components.[43] DECT has been widely used to measure LN size in assessing the prognosis of patients with advanced cancer.[16,36,44] Additionally, DECT

can effectively eliminate the interference of prosthetic metal artifacts during imaging, making it easier to observe the soft tissues around joint prostheses, especially the LNs. More importantly, DECT offers rapid CT imaging with fewer contraindications. This non-invasive and cost-effective method is more acceptable to patients and easier to implement in clinical practice.

This study has several limitations. The exclusion criteria may limit the generalizability of our findings. Patients with conditions such as skin ulcers, recent trauma, or inflammatory diseases were excluded, which may not fully represent the broader population undergoing joint revision surgery. In this study, we employed strategies such as multi-site sampling, repeated cultures, extended culture durations, and combined diagnostic methods to minimize false negatives and contamination in pathogen detection. However, we acknowledge that relying solely on pathogen culture results as a diagnostic standard does not completely eliminate the risks of false positives or negatives. Like the MSIS and ICM criteria, current diagnostic methods remain imperfect.[8] Therefore, future studies will aim to align our findings with international consensus diagnostic standards to ensure their reliability and clinical applicability. Inflammatory diseases can also affect LNs, potentially reducing the accuracy of our method. In future studies, we aim to explore the differential presentation of external iliac LNs in patients with inflammatory diseases compared to those with PJI. Additionally, this study was conducted at a single center with a relatively small sample size, requiring larger multicenter studies for further validation. Although DECT has significant advantages for imaging LNs, operator handling and interpretation could introduce bias. Therefore, in our study, we standardized measurements among experienced radiologists, validated inter-rater consistency, and obtained average values to enhance the credibility of our findings. This study focused on LN size, which may overlook other important factors contributing to the pathophysiology of PJI, such as variations in immune responses among patients or specific pathogens involved. Focusing solely on the long or short axis of LNs in the context of infection may be confounded by atypical LNs, such as spindle-shaped nodes.[36] Therefore, using a combined approach of long and short axis measurements improved the accuracy of the method in our study. Studies have shown that imaging markers of lymph nodes during disease onset and progression include contour deformation, abnormal enhancement, and size changes.[45] In our study, we focused on the size of the external iliac lymph nodes, finding that changes in the long and short axes demonstrated potential for diagnosing PJI. However, we did not investigate whether other lymph node characteristics are altered in the context of PJI. Considering the challenges posed by irregular lymph node morphology and interference from surrounding tissues on the accuracy of three-dimensional measurements, as well as the lack of established clinical methods for lymph node volume measurement, our study did not explore changes in lymph node volume in PJI. Nonetheless, lymph node volume remains a potentially valuable imaging feature worth further investigation. Previous research has shown that increased uptake of 18F-fluorodeoxyglucose in inguinal lymph nodes aids in diagnosing fracture-related infections.[46] Therefore, incorporating other lymph node imaging characteristics and combining different imaging techniques may further enhance the accuracy and robustness of lymph node-based diagnostics for PJI. Additionally, utilizing reliable imaging features and leveraging artificial intelligence to integrate and analyze multimodal imaging characteristics represent important directions for future research to optimize diagnostic models. Finally, DECT is more expensive than conventional single-energy CT, increasing the financial burden on patients. In resource-limited settings, the availability and expertise required to perform and interpret DECT scans may limit its practical application. However, our study demonstrates that DECT is highly effective for diagnosing PJI and serves as a reliable, non-invasive, and rapid diagnostic tool. Compared to the labor-intensive testing of multiple serum and synovial biomarkers, DECT iodine imaging also offers certain economic advantages, providing patients with an alternative diagnostic option.

Conclusion

This study demonstrates that DECT can detect volume changes in the external iliac LNs on the affected side in PJI patients during infection. It also allows for the determination of diagnostic thresholds based on the maximum long and short axis diameters, offering high diagnostic value and an effective new method for early PJI diagnosis. We believe that DECT measurement of external iliac LN size is a reliable, rapid, and non-invasive diagnostic method. The application of this technique is expected to improve the PJI diagnostic process, enhance treatment outcomes, and improve patient prognosis.

Ethical Approval

All procedures involving human participants in this study were conducted in accordance with the ethical standards of the Institutional Research Committee of the First Affiliated Hospital of Chongqing Medical University (No. 2021-258) and the ethical standards of the Chinese Clinical Trial Registry (No. ChiCTR2100050785). This study adhered to the ethical principles outlined in the Declaration of Helsinki. Individual deidentified participant data can be obtained upon request from Professor Leilei Qi.

Informed Consent

Informed consent was obtained from all individual participants included in the study.

Acknowledgments

This study used ChatGPT4.0 to assist the author in improving the language of the first draft after its completion, in order to enhance the fluency and readability of the text. However, the accuracy of the content, viewpoints, and responsibility for the final article are assumed by the author.

Author Contributions

Wei Huang and Leilei Qin contributed equally to this work and should be considered as equal corresponding authors. All authors made a significant contribution to the work reported, whether that is in the conception, study design, execution, acquisition of data, analysis and interpretation, or in all these areas; took part in drafting, revising or critically reviewing the article; gave final approval of the version to be published; have agreed on the journal to which the article has been submitted; and agree to be accountable for all aspects of the work.

Funding

This work was funded by Natural Science Foundation of Chongqing, China (Grant No. CSTB2024NSCQ-MSX0921) and National Natural Science Foundation of China (Grant No. 82402836). The corresponding author, Leilei Qin, received support from these funding sources.

Disclosure

The authors have not disclosed any competing interests.

References

1. Parvizi J, Tan TL, Goswami K, et al. The 2018 definition of periprosthetic hip and knee infection: an evidence-based and validated criteria. *J Arthroplasty*. 2018;33(5):1309–1314.e2. doi:10.1016/j.arth.2018.02.078
2. Peng K-T, Chiang Y-C, Huang T-Y, Chen P-C, Chang P-J, Lee C-W. Curcumin nanoparticles are a promising anti-bacterial and anti-inflammatory agent for treating periprosthetic joint infections. *Int J Nanomed*. 2019;14:469–481. doi:10.2147/IJN.S191504
3. Navarro G, Lozano L, Sastre S, Bori R, Bosch J, Bori G. Experiences during switching from two-stage to one-stage revision arthroplasty for chronic total knee arthroplasty infection. *Antibiotics*. 2021;10(12):1436. doi:10.3390/antibiotics10121436
4. Fillerova R, Gallo J, Radvansky M, Kraiczova V, Kudelka M, Kriegova E. Excellent diagnostic characteristics for ultrafast gene profiling of DEFA1-IL1B-LTF in detection of prosthetic joint infections. *J Clin Microbiol*. 2017;55(9):2686–2697. doi:10.1128/JCM.00558-17
5. Su X, Chen Y, Zhan Q, et al. The Ratio of IL-6 to IL-4 in synovial fluid of knee or hip performances a noteworthy diagnostic value in prosthetic joint infection. *J Clin Med*. 2022;11(21):6520. doi:10.3390/jcm11216520
6. Qin L, Hu N, Zhang Y, et al. Antibody-antibiotic conjugate targeted therapy for orthopedic implant-associated intracellular s. aureus infections. *J Adv Res*. 2023;S2090123223003752. doi:10.1016/j.jare.2023.12.001
7. Parvizi J, Zmistowski B, Berbari EF, et al. New definition for periprosthetic joint infection: from the workgroup of the musculoskeletal infection society. *Clin Orthop Relat Res*. 2011;469(11):2992–2994. doi:10.1007/s11999-011-2102-9
8. Tripathi S, Tarabichi S, Parvizi J, Rajgopal A. Current relevance of biomarkers in diagnosis of periprosthetic joint infection: an update. *Arthroplasty*. 2023;5(1):41. doi:10.1186/s42836-023-00192-5
9. Baek YJ, Lee Y-J, Lee JA, et al. Role of α-Defensin and the Microbiome in Prosthetic Joint Infection: a Prospective Cohort Study in Korea. *J Clin Med*. 2023;12(18):5964. doi:10.3390/jcm12185964
10. Qin L, Du C, Yang J, et al. Synovial fluid interleukin levels cannot distinguish between prosthetic joint infection and active rheumatoid arthritis after hip or knee arthroplasty. *Diagnostics (Basel)*. 2022;12(5):1196. doi:10.3390/diagnostics12051196
11. Riedel A, Helal M, Pedro L, et al. Tumor-derived lactic acid modulates activation and metabolic status of draining lymph node stroma. *Cancer Immunol Res*. 2022;10(4):482–497. doi:10.1158/2326-6066.CIR-21-0778
12. Schaeuble K, Cannelle H, Favre S, et al. Attenuation of chronic antiviral t-cell responses through constitutive COX2-dependent prostanoid synthesis by lymph node fibroblasts. *PLoS Biol*. 2019;17(7):e3000072. doi:10.1371/journal.pbio.3000072

13. Shimono J, Miyoshi H, Kamimura T, et al. Clinicopathological features of primary splenic follicular lymphoma. *Ann Hematol*. 2017;96 (12):2063–2070. doi:10.1007/s00277-017-3139-y
14. Buettner M, Bode U. Lymph node dissection--understanding the immunological function of lymph nodes. *Clin Exp Immunol*. 2012;169 (3):205–212. doi:10.1111/j.1365-2249.2012.04602.x
15. T H, A A, Am R, H A. Intra-mammary lymph nodes, an overlooked breast cancer prognostic tool? *World J Surg Oncol*. 2021;19(1):1. doi:10.1186/s12957-021-02219-0
16. You Y, Wang Y, Yu X, et al. Prediction of lymph node metastasis in advanced gastric adenocarcinoma based on dual-energy ct radiomics: focus on the features of lymph nodes with a short axis diameter ≥6 mm. *Front Oncol*. 2024;14:1369051. doi:10.3389/fonc.2024.1369051
17. Qin L, Zhao C, Wang H, et al. Detection of inguinal lymph nodes is promising for the diagnosis of periprosthetic joint infection. *Front Cell Infect Microbiol*. 2023;13:1129072. doi:10.3389/fcimb.2023.1129072
18. Bui T, Bordoni B. *Anatomy, Abdomen and Pelvis: Inguinal Lymph Node*. StatPearls; StatPearls Publishing: Treasure Island (FL); 2024.
19. Gray's Anatomy Elsevier. elsevier.com. Available from:https://www.elsevier.com/books-and-journals/book-series/grays-anatomy. Accessed August 8, 2024.
20. Isern-Kebschull J, Tomas X, García-Díez AI, Morata L, Ríos J, Soriano A. Accuracy of computed tomography–guided joint aspiration and computed tomography findings for prediction of infected hip prosthesis. *J Arthroplasty*. 2019;34(8):1776–1782. doi:10.1016/j.arth.2019.04.018
21. Romanò CL, Petrosillo N, Argento G, et al. The role of imaging techniques to define a peri-prosthetic hip and knee joint infection: multidisciplinary consensus statements. *J Clin Med*. 2020;9(8):2548. doi:10.3390/jcm9082548
22. Busch A, Jäger M, Beck S, et al. Metal artefact reduction sequences (mars) in Magnetic Resonance Imaging (MRI) after Total Hip Arthroplasty (THA): a Non-Invasive Approach for Preoperative Differentiation between Periprosthetic Joint Infection (PJI) and Aseptic Complications? *BMC Musculoskelet Disord*. 2022;23(1):620. doi:10.1186/s12891-022-05560-x
23. Nie L, Sun Z, Shan F, Li C, Ding X, Shen C. An artificial intelligence framework for the diagnosis of prosthetic joint infection based on 99mTc-MDP dynamic bone scintigraphy. *Eur Radiol*. 2023;33(10):6794–6803. doi:10.1007/s00330-023-09687-w
24. Tande AJ, Patel R. Prosthetic Joint Infection. *Clin Microbiol Rev*. 2014;27(2):302–345. doi:10.1128/CMR.00111-13
25. Yue D, Fan Rong C, Ning C, et al. Reduction of metal artifacts from unilateral hip arthroplasty on dual-energy CT with metal artifact reduction software. *Acta Radiol*. 2018;59(7):853–860. doi:10.1177/0284185117731475
26. Li Z, Ravishankar S, Long Y, Fessler JA. DECT-MULTRA: dual-energy CT image decomposition with learned mixed material models and efficient clustering. *IEEE Trans Med Imaging*. 2020;39(4):1223–1234. doi:10.1109/TMI.2019.2946177
27. Cheng Q, Yang Y, Li F, Li X, Qin L, Huang W. Dual-energy computed tomography iodine maps: application in the diagnosis of periprosthetic joint infection in total hip arthroplasty. *J Arthroplasty*. 2024;S0883–5403(24)00811–8. doi:10.1016/j.arth.2024.08.007
28. Aldrich M, Hall M, Angermiller B, Robinson H, Sevick-Muraca E. Systemic decrease in murine collecting vessel lymphatic function during initial stages of inflammation (110.5). *J Immunol*. 2011;186(1_Supplement):110.5. doi:10.4049/jimmunol.186.Supp.110.5
29. Ghirardelli ML, Jemos V, Gobbi PG. Diagnostic Approach to Lymph Node Enlargement. *Haematologica*. 1999;84(3):242–247.
30. Slap GB, Brooks JS, Schwartz JS. When to perform biopsies of enlarged peripheral lymph nodes in young patients. *JAMA*. 1984;252 (10):1321–1326. doi:10.1001/jama.1984.03350100051031
31. Bazemore AW, Smucker DR. Lymphadenopathy and Malignancy. *Am Fam Physician*. 2002;66(11):2103–2110.
32. Ji B, Aimaiti A, Wang F, et al. Intraoperative direct sonication of implants and soft tissue for the diagnosis of periprosthetic joint infection. *J Bone Joint Surg*. 2023;105(11):855–864. doi:10.2106/JBJS.22.00446
33. Koo TK, Li MY. A guideline of selecting and reporting intraclass correlation coefficients for reliability research. *J Chiropr Med*. 2016;15 (2):155–163. doi:10.1016/j.jcm.2016.02.012
34. McNally M, Sousa R, Wouthuyzen-Bakker M, et al. The EBJIS definition of periprosthetic joint infection. *Bone Joint J*. 2021;103-B(1):18–25. doi:10.1302/0301-620X.103B1.BJJ-2020-1381.R1
35. Zhou H, Yang Y, Zhang Y, et al. Current status and perspectives of diagnosis and treatment of periprosthetic joint infection. *Infect Drug Resist*. 2024;17:2417–2429. doi:10.2147/IDR.S457644
36. Wang D, Zhuang Z, Wu S, et al. A dual-energy ct radiomics of the regional largest short-axis lymph node can improve the prediction of lymph node metastasis in patients with rectal cancer. *Front Oncol*. 2022;12:846840. doi:10.3389/fonc.2022.846840
37. Hicks DG, Judkins AR, Sickel JZ, Rosier RN, Puzas JE, O'keefe RJ. Granular histiocytosis of pelvic lymph nodes following total hip arthroplasty. the presence of wear debris, cytokine production, and immunologically activated macrophages*. *J Bone Joint Surg*. 1996;78(4):482–496. doi:10.2106/00004623-199604000-00002
38. Parvizi J, Gehrke T. International consensus group on periprosthetic joint infection. definition of periprosthetic joint infection. *J Arthroplasty*. 2014;29(7):1331. doi:10.1016/j.arth.2014.03.009
39. Qin L, Li X, Wang J, Gong X, Hu N, Huang W. Improved diagnosis of chronic hip and knee prosthetic joint infection using combined serum and synovial IL-6 tests. *Bone Joint Res*. 2020;9(9):587–592. doi:10.1302/2046-3758.99.BJR-2020-0095.R1
40. Qin L, Hu N, Li X, Chen Y, Wang J, Huang W. Evaluation of synovial fluid neutrophil CD64 index as a screening biomarker of prosthetic joint infection. *Bone Joint J*. 2020;102-B(4):463–469. doi:10.1302/0301-620X.102B4.BJJ-2019-1271.R1
41. Van den Wyngaert T, Strobel K, Kampen WU, et al. Joint committee and the oncology committee. The EANM practice guidelines for bone scintigraphy. *Eur J Nucl Med Mol Imaging*. 2016;43(9):1723–1738. doi:10.1007/s00259-016-3415-4
42. Karmazyn B, Supakul N, Lehnert SJ, et al. Retroperitoneal and pelvic lymph nodes in children: what is normal? *Am J Roentgenol*. 2020;214 (6):1384–1388. doi:10.2214/AJR.19.22316
43. Petrongolo M, Zhu L. Noise suppression for dual-energy CT through entropy minimization. *IEEE Trans Med Imaging*. 2015;34(11):2286–2297. doi:10.1109/TMI.2015.2429000
44. Li S, Wei X, Wang L, et al. Dual-source dual-energy ct and deep learning for equivocal lymph nodes on ct images for thyroid cancer. *Eur Radiol*. 2024. doi:10.1007/s00330-024-10854-w
45. Ramirez M, Ingrand P, Richer J-P, et al. What is the pelvic lymph node normal size? Determination from normal MRI examinations. *Surg Radiol Anat*. 2016;38(4):425–431. doi:10.1007/s00276-015-1581-x
46. Wang Y, Sun Z, Liang X, Shen C. Inguinal draining-lymph node in 18F-FDG PET/CT images could be a new indicator for the diagnosis of fracture-related infection in the lower extremities. *Front Immunol*. 2023;14. doi:10.3389/fimmu.2023.1206682.